Wave-packet dynamics for general contact interactions on a circular setup: Revivals, bouncing, and trapping

Alexandre G. M. Schmidt* and M. G. E. da Luz†
Departamento de Física, Universidade Federal do Paraná, Caixa Postal 19044, 81531-990 Curitiba, PR, Brazil
(Received 23 December 2003; published 12 May 2004)

Here we study a one-dimensional finite lattice formed by generalized contact interactions in a circular setup, i.e., under periodic boundary conditions. Considering only four such potentials, we show the emergence of different behaviors as revivals, bouncing, and trapping for the time evolution of wave packets. This is done by properly choosing the parameters that characterize the contact interactions. We also discuss possible physical applications for this type of system, such as using it to split an initially localized state into spatially separated and dynamically independent parts.

DOI: 10.1103/PhysRevA.69.052708 PACS number(s): 03.65.Nk, 03.65.Ge, 03.65.Db

I. INTRODUCTION

The wavelike characteristics of the quantum world lead to countless unexpected phenomena at the microscopic scales. To control these phenomena by driving the time evolution of quantum states has become a very active research area of both fundamental and practical importance (see, for instance, the overview in Ref. [1]). Probably the most straightforward way of all to achieve quantum control is just to find (or build) specific systems that, by adjusting appropriate parameters, can behave as we wish.

A particularly rich problem is the one of wave-packet scattering by multiple barrier potentials [2]. Even in very simple situations interesting effects, such as *revivals, bouncing*, and *trapping* can take place. Indeed, if we put a Gaussian wave packet inside an infinite one-dimensional (1D) well, the packet will spread and fill all the allowed space. However, after a time T_f (partial revival) it will start to reconstruct itself, returning to its original shape after an elapsed revival time T_r [3]. The so called super-revival can also be seen in finite square-well potentials [4,5]. Quantum revivals are present in different contexts like quantum computation [6]; the classical-quantum correspondence in Rydberg atoms [7]; anharmonic vibrational potentials [8]; femtosecond dynamics in physics and chemistry [9]; and many others [10,11]. Bouncing is when a quantum state oscillates between only two spatially separated regions, as in resonant coupling between two particular single wells of a multiple well potential. Finally, by trapping we mean that the wave packet stays confined in a particular region of the configuration space, not evolving to the other energetically allowed regions. As examples we cite suppression of tunneling from one side to the other for a wave packet in a double well constituted of a rectangular barrier [12] or a δ potential [13] within an infinite square well; and eigenstate localization for a starlike quantum graph [14]. It is important to note that such behavior is not associated with Anderson localization, since no disorder is involved.

In a recent work [15], the problem of a 1D lattice (periodic or not) of N arbitrary contact interactions was discussed in general terms and also the many possible physical applications for it. Contact interactions are idealizations of very short range potentials, which have the effect of imposing different boundary conditions on the system wave function at the potential locations. They are very useful in developing analytical models to study complicated processes, such as ion-atom collisions [16], many-body interactions [17], fermion-boson duality [18], and regularization schemes [19].

In this contribution we show that, by properly setting the contact interaction parameter values, quite simple configurations of the lattices mentioned above can exhibit revivals, bouncing, and trapping. We work with a finite 1D lattice of length L, having just four general contact interactions arbitrarily located along it. We assume a circular setup, i.e., periodic boundary conditions where $x=0\equiv x=L$ (which we will call a circle, for short). Our particular choice of four potentials is just because it is a simple case that already displays all the aspects we shall discuss.

Although this paper deals with a theoretical analysis of a model system, it may be of concrete interest (and conceivably be implemented) in actual laboratory conditions. This is so because, first, general contact interactions can be constructed as a composition of δ potentials [20], which in their turn are in principle realizable from some well behaved short-range potentials, as in the case of sharp quantum walls [21]. Second, a series of works by Stöckmann and collaborators [22] studies 1D circular arrangements for microwave scattering, whose dynamics are analogous to the present systems. So our predictions eventually could be investigated in such experiments.

The outline of the paper is as follows. In Sec. II we establish our systems, presenting their eigenfunctions, eigenvalues, and the construction of wave packets. In Sec. III, we calculate the wave-packet time evolution for different contact interactions on the circle and discuss the emergence of revivals, bouncing, and trapping. Finally, in Sec. IV we present our final remarks and conclusion.

II. THE SYSTEM

A. Eigenvalues and eigenfunctions

The Schrödinger equation of the problem is simply $[d^2/dx^2+k^2]\phi(x)=0$, with x in the interval $[0,L]$ and $0\equiv L$.

*Electronic address: schmidt@fisica.ufpr.br
†Electronic address: luz@fisica.ufpr.br

The effect of the four generalized contact interactions (located at l_j, with $0<l_1<l_2<l_3<l_4<L$) is represented by a set of boundary conditions imposed on ϕ at these l_j's. Throughout the paper we use the natural units $\hbar=2m=1$, so all the plotted quantities will be dimensionless.

Let an eigenfunction in the region $l_{j-1}<x<l_j$ ($j=1,\ldots,5, l_0=0, l_5=L$) be written as

$$\phi_j(x) = A_j \sin(kx) + B_j \cos(kx). \tag{1}$$

From self-adjoint extensions, we know that the most general contact interaction at l_j can be represented by [23]

$$\begin{pmatrix} \phi_{j+1}(l_j) \\ \phi'_{j+1}(l_j) \end{pmatrix} = \exp[i\theta_j] \begin{pmatrix} a_j & b_j \\ c_j & d_j \end{pmatrix} \begin{pmatrix} \phi_j(l_j) \\ \phi'_j(l_j) \end{pmatrix}, \quad j=1,\ldots,4. \tag{2}$$

Here, $f'(x)=df(x)/dx$ and $a_jd_j-b_jc_j=1$, with a_j,b_j,c_j,d_j, and θ_j being real parameters which define each contact interaction at $x=l_j$. Finally, due to the periodic boundary conditions (circle case) we must impose $\phi_1(0)=\phi_5(L)$ and $\phi'_1(0)=\phi'_5(L)$.

The coefficients A and B are linked through a homogeneous system of ten equations plus the normalization condition. By solving it we get the eigenfunctions as well as the quantization condition $g(k)=0$ in terms of the 20 parameters $\{a_j,b_j,c_j,d_j\}$ and $\{\theta_j\}$. The exact general expressions for the coefficients and for $g(k)$ are very cumbersome and we will not write them down here. Just as an illustration, we quote the $g(k)$ for two simple cases. When the four contact interactions are the usual δ potential and all having the same strength γ, the eigenvalue $E_n=k_n^2$ is obtained as the nth root of the transcendental equation

$$\begin{aligned} g_\delta(k) = {} & 16k^4(\cos[kL]-1) + \gamma^2(\gamma^2-24k^2)\cos(kL) - \gamma^2(\gamma^2 \\ & -4k^2)C_1(k) + \gamma^2(\gamma^2+4k^2)C_2(k) + \gamma^4\cos[k(L+2\ell)] \\ & -8\gamma k(\gamma^2-4k^2)\sin(kL) + 4\gamma^3 k S_1(k), \end{aligned} \tag{3}$$

where $\ell=l_1-l_2+l_3-l_4$, and

$$\begin{aligned} C_1(k) = {} & \cos[k(L+2l_1-2l_2)] + \cos[k(L+2l_2-2l_3)] \\ & + \cos[k(L+2l_3-2l_4)] + \cos[k(L+2l_4-2l_1)], \end{aligned}$$

$$C_2(k) = \cos[k(L+2l_1-2l_3)] + \cos[k(L+2l_2-2l_4)],$$

$$\begin{aligned} S_1(k) = {} & \sin[k(L+2l_1-2l_2)] + \sin[k(L+2l_2-2l_3)] \\ & + \sin[k(L+2l_3-2l_4)] - \sin[k(L+2l_1-2l_4)]. \end{aligned} \tag{4}$$

For the case where the contact interactions are four δ' potentials (see next section), also of equal strength γ, we have

$$\begin{aligned} g_{\delta'}(k) = {} & k^4(\{16(1-\cos[kL]) + (24\gamma^2k^2-\gamma^4k^4)\cos(kL)\} \\ & + \gamma^2k^2(\gamma^2k^2-4)C_1(k) - \gamma^2k^2(\gamma^2k^2+4)C_2(k) \\ & - \gamma^4k^4\cos(k[L+2\ell]) + 4\gamma^3k^3S_1(k)). \end{aligned} \tag{5}$$

B. Time evolution

To study the time evolution of wave packets, we use the standard approach of writing $\psi(x,t)$ in terms of the eigenfunctions $\{\phi^{(n)}\}$ of the problem, or $\psi(x,t)=\Sigma_n c_n \times \exp[-ik_n^2t]\phi^{(n)}(x)$. Here, the c_n's are the expansion coefficients of the initial state, given by $c_n=\int_0^L dx\ \psi(x,0)\phi^{(n)^*}(x)$. In practice, the sum over n is truncated at a certain $n=N$, whose value determines the numerical precision for the series in representing ψ. Unless otherwise mentioned, for the initial wave packets we consider expansions that closely fit the Gaussian

$$\psi(x,0) = \frac{1}{(2\pi)^{1/4}\Delta_0^{1/2}} \exp\left[ik_0x - \frac{(x-x_0)^2}{4\Delta_0^2}\right]. \tag{6}$$

For the L's, x_0, and Δ_0 we are going to use in the examples, Eq. (6) is practically null at $x=0$ and $x=L$; therefore the fact that $\phi^{(n)}(0)=\phi^{(n)}(L)$ for all n does not become a problem in constructing the expansions. Moreover, for such parameter values $\int_0^L dx\ \psi(x,0)\psi(x,0)^*=1$, with the numerical error being irrelevant, always less than 10^{-20}.

III. WAVE-PACKET PROPAGATION

Using the expansions as described before, we assume different conditions for our four contact interactions and then analyze some features of the wave-packet propagation on the circle. For the latter purpose we observe that for a single contact interaction on the line $(-\infty,+\infty)$, placed at the origin and characterized by the boundary conditions (2), the reflection and transmission amplitudes for a plane wave of wave number k and incident either from left $(+)$ or right $(-)$ are given by [15]

$$R^{(\pm)} = \frac{c \pm ik(d-a) + bk^2}{-c + ik(d+a) + bk^2}, \quad T^{(\pm)} = \frac{2ik\exp[\pm i\theta]}{-c + ik(d+a) + bk^2}. \tag{7}$$

Hereafter we call the intervals $l_1<x<l_2$, $l_2<x<l_3$, and $l_3<x<l_4$, respectively, regions II, III, and IV. Recalling the periodic boundary conditions, we have that the intervals $0<x<l_1$ and $l_4<x<L$ form in fact the single region I. Regarding the wave-packet parameters, in all the calculations we set $\Delta_0=0.07$ and $x_0=(l_1+l_2)/2$, so the initial wave packet (6) is always in the middle of region II.

In the following we show the emergence of different phenomena such as revival, bouncing, and trapping.

A. δ potentials

The simplest case is four δ interactions of the same strength γ, which are obtained from Eq. (2) by letting $a=d=1$, $b=\theta=0$, and $c=\gamma$. In all the calculations here we use $N=102$, leading to a precision for the initial wave packet better than 10^{-10}, i.e., $\int_0^L dx|\psi(x,0)-\Sigma_{n=1}^{n=N}c_n\phi^{(n)}(x)|^2<10^{-10}$.

We start by choosing $\gamma=120$ and $k_0=0$ for the initial wave packet. Consider then $l_1=1$, $l_2=1+\sqrt{2}$, $l_3=2.1+\sqrt{2}$, $l_4=2.1+2\sqrt{2}$, and $L=5$, so that the region lengths are $L_I=1.07$, $L_{II}=\sqrt{2}$, $L_{III}=1.1$, and $L_{IV}=\sqrt{2}$. For these parameters, we plot in

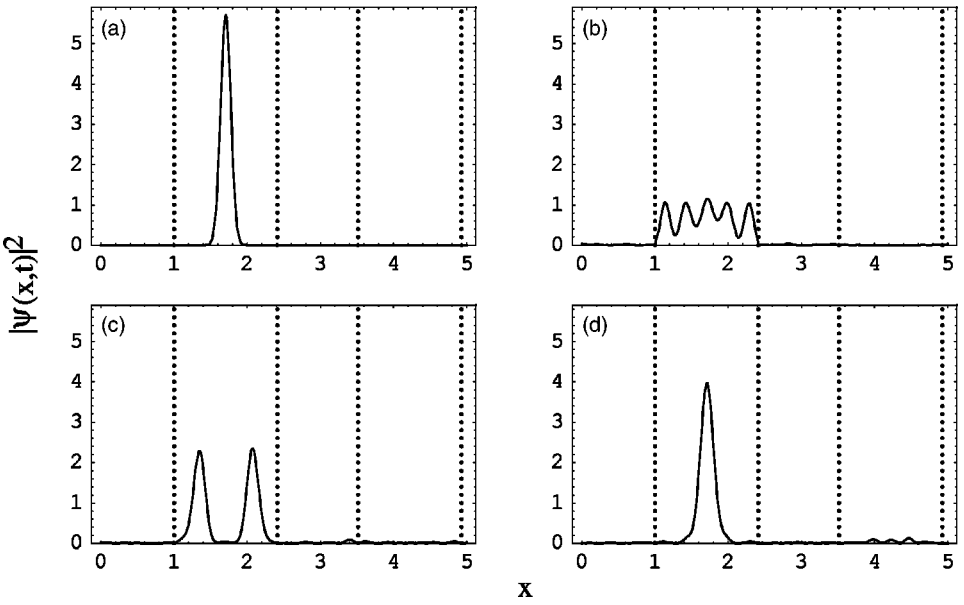

FIG. 1. The time evolution of the Gaussian wave packet, Eq. (6), for the situation as in the text. Here is shown $|\psi(x,t)|^2$ as a function of x for the following short values for the time: (a) $t=0$; (b) $t=0.132$; (c) $t=0.574$; and (d) $t=0.82$. Observe the partial and (almost) full revival inside region II.

Fig. 1 $|\psi(x,t)|^2$ versus x for some small values of t. At this time scale the particle essentially does not tunnel to the other regions, remaining at region II where we can observe partial and full revivals [see Figs. 1(c) and 1(d)]. For larger times ($t>20$), however, the wave packet can leave region II, but evolving only to region IV, bouncing back and forth, Fig. 2. The joint probability for the particle to be found in regions I and III is always quite small, never exceeding 4%, which we have verified numerically for times up to $t=3000$.

Note that in the above example $L_{II}=L_{IV}$ are incommensurable with both L_I and L_{III}. This condition associated with the strengths values of the δ's prevents the wave packet from evolving to regions I and III. Bearing this fact in mind, we can construct other setups where the probability density remains very high within just one of the four regions, say, region II. For instance, consider the case of $l_1=0.8$, $l_2=0.8+\sqrt{3}$, $l_3=1.7+\sqrt{3}$, and $l_4=1.7+\sqrt{2}+\sqrt{3}$, keeping all the other parameter values. We find that indeed the particle is trapped, never leaving region II, so that $\int_{l_1}^{l_2}|\psi(x,t)|^2dx$ is practically equal to 1 for all t (solid curve in Fig. 3).

An interesting point is to determine how the different regions are *dynamically disconnected* when we have trapping. To analyze it, we consider at $t=0$ a wave packet that is 50% in region II and 50% in region IV, or

$$\psi(x,0)=\frac{\sqrt{2}}{(2\pi)^{1/4}\Delta_0^{1/2}}\left(\exp\left[ik_0x-\frac{(x-x_0)^2}{4\Delta_0^2}\right]+\exp\left[ik_0x-\frac{(x-x_0')^2}{4\Delta_0^2}\right]\right). \tag{8}$$

Here, $x_0'=(l_3+l_4)/2$ is the middle position of region IV. In Fig. 3 we compare the time evolutions of Eqs. (6) and (8) (note that for a better comparison, the above wave packet is normalized to 2). From the plots we see that the evolution of the left part of Eq. (8) is very similar to the evolution of Eq.

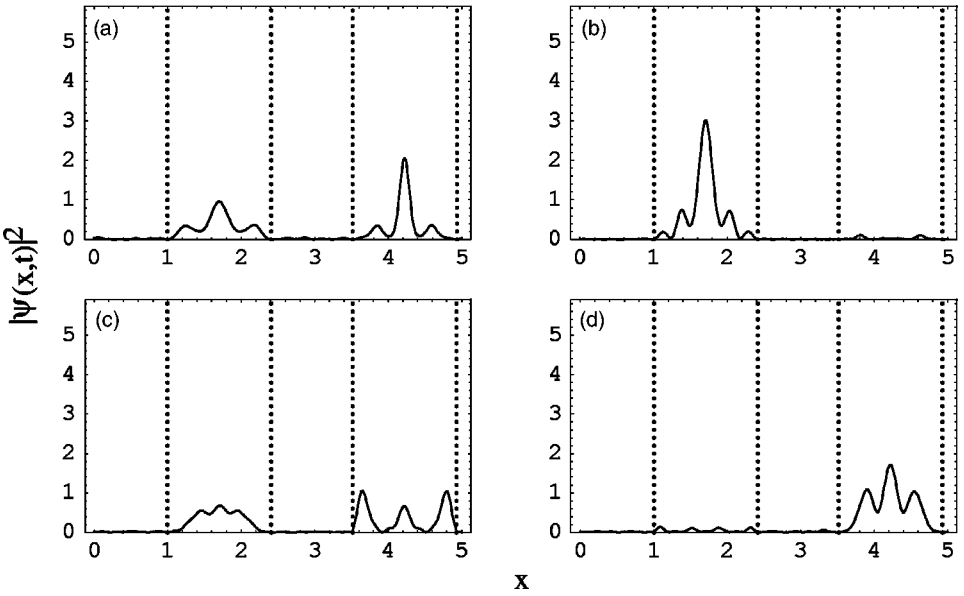

FIG. 2. The same as in Fig. 1 for the times (a) $t=72$; (b) $t=1083.08$; (c) $t=1108$; and (d) $t=1440$.

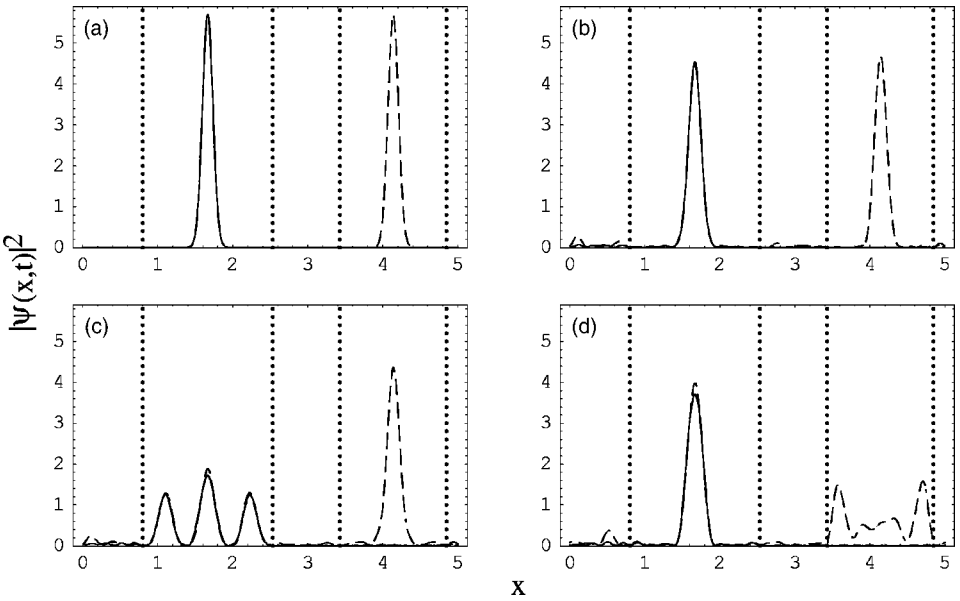

FIG. 3. $|\psi(x,t)|^2$ versus x, where $\psi(x,0)$ is the initial wave packet given in Eq. (6) (solid curve) and in Eq. (8) (dashed curve) for the parameters given in the text. Here (a) $t=0$; (b) $t=0.487$; (c) $t=505.04$; and (d) the very long $t=14\,400.948$.

(6). This shows that the two halves of Eq. (8) evolve fairly independently, each trapped in its initial region.

From the results so far, we shall make some remarks. By choosing different parameter values for this very simple system composed of four δ potentials within a circle, we can "drive" the initial Gaussian wave packet to (a) spread over the whole circle (just by having all the contact interactions equally spaced); (b) tunnel back and forth between only two regions, which do not need to be neighbors; or (c) stay confined within one single region. Thus, in principle such devices could be used to generate spatially separated Schrödinger's cats [24]. In fact, we could start with a situation like that of Fig. 2. After some time the initial state would evolve to a 50-50 probability in two distinct regions. Then, by an appropriate sudden change in one of the δ positions, we could split the wave packet into two parts, each locked within its own region, as in Fig. 3.

Such state separation is particularly interesting if the two parts are far away from each other, as in the case of "mirages" in quantum corrals [25,26]. In [25], the electronic states surrounding a single magnetic Co atom deposited on a Cu (111) surface are placed on the focus of a quantum corral in the shape of an ellipse. Due to interference effects, these states appear on the second focus, a phenomenon called quantum mirage. In the experiments, the distance between the states and their image is roughly about ten times the characteristic size of the electronic states around the Co atom. Motivated by those results, we ask if we can also obtain such separations in our much simpler problem. So we consider four δ interactions all with the same strength $\gamma=240$. We assume that regions I and IV have lengths 13.1 and 13, respectively. For regions II and IV, we assume (a) $L_{II}=L_{IV}=\sqrt{2}$, and (b) $L_{II}=\sqrt{3}$ and $L_{IV}=\sqrt{2}$. Thus, regions I and III are about ten times larger than regions II and IV. For the situation (a) the wave packet predominantly bounces between the regions II and IV. For this case we plot in Fig. 4(a) $P_{II,IV}=\int_{l_1}^{l_2}|\psi(x,t)|^2dx+\int_{l_3}^{l_4}|\psi(x,t)|^2dx$ as a function of time. The probability of the particle staying in these two regions is never inferior to 88%, a reasonable result. When the lengths L_{II} and L_{IV} are distinct and irrational, case (b), the wave packet stays in region II, not evolving to the other three. The trapping is better than 94% as shown in Fig. 4(b), where we plot $P_{II}=\int_{l_1}^{l_2}|\psi(x,t)|^2dx$ as a function of t.

Finally, we report for the δ case how much we can change the parameters and yet have the wave packet confined within a single region. Considering the parameter values of Fig. 3, by keeping $k_0=0$ if we decrease γ we see that for $\gamma=40$ the particle still stays trapped in a single region. On the other hand, by fixing $\gamma=120$, the confinement takes place for k_0 up to 9. We also discuss the incommensurability condition. For the results shown in Figs. 1–3, the square roots are in fact taken to seven decades. However, by using $\sqrt{2}\approx 1.414$ and

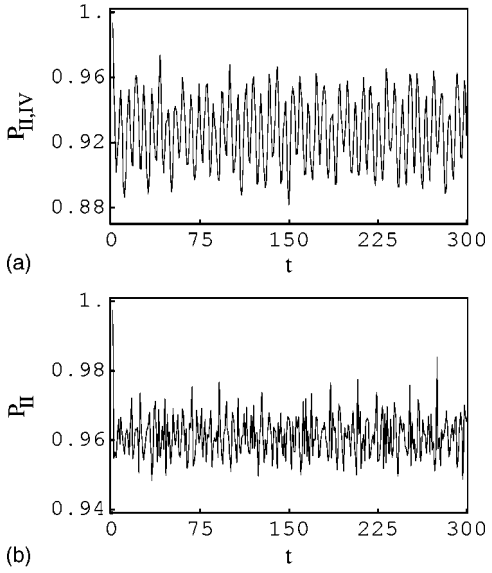

FIG. 4. (a) $P_{\mathrm{II,IV}}=\int_{l_1}^{l_2}|\psi(x,t)|^2dx+\int_{l_3}^{l_4}|\psi(x,t)|^2dx$ for $L_{II}=L_{III}=\sqrt{2}$ and (b) $P_{\mathrm{II}}=\int_{l_1}^{l_2}|\psi(x,t)|^2dx$ for $L_{II}=\sqrt{3}$ and $L_{III}=\sqrt{2}$ as functions of t (time calculated in steps of ten units, the continuous line being just for better visualization) and the other parameters as in the text. It should be mentioned that these oscillation patterns do not change for larger times.

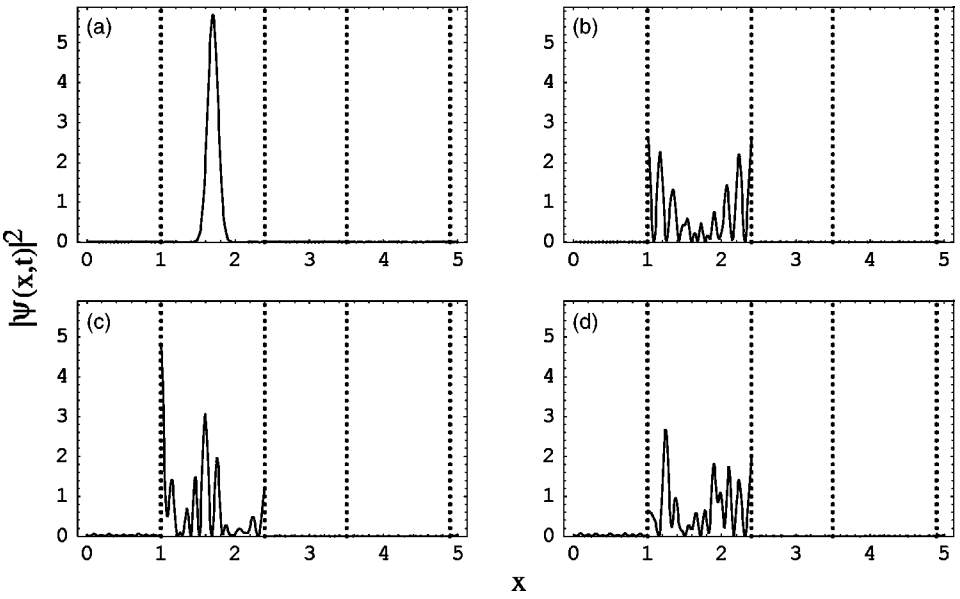

FIG. 5. $|\psi(x,t)|^2$ as function of x for the configuration $\delta'-\delta'-\delta-\delta'$ and the parameter values as in the text. Here, the times are (a) $t=0$; (b) $t=0.955$; (c) $t=5000$; (d) $t=25\,000$. We see that the wave packet does not escape from its initial region II. The discontinuities of the wave packet are a consequence of the δ' potentials located at $x=l_1$ and $x=l_2$.

$\sqrt{3}\approx 1.732$ we find for all the previous examples essentially the same behaviors of bouncing and trapping. The difference is that now the wave packets do not evolve exactly in the same way, e.g., the revival times have different values. By further approximating the square roots to only two decades, we see some "leakage," which nevertheless is small. For instance, for the same parameters as in Fig. 3, the probability for the particle to be outside region II never exceeds 5%.

B. δ' potentials

The so-called delta-prime interaction, δ', despite the name is not merely the derivative of the usual delta function [27]. If it is placed at $x=l$, then the resulting wave function becomes discontinuous at $x=l$, but with the first derivative remaining continuous. A δ' of coupling constant γ is obtained from Eq. (2) by letting $a=d=1$, $b=\gamma$, $c=\omega=0$. Here we quote the quantum amplitudes for a single δ' on the full line Eq. (7): $R^{(\pm)}=R=\gamma k/[2i+\gamma k]$ and $T^{(\pm)}=T=2i/[2i+\gamma k]$.

The first point to observe is that, in order to build a Gaussian wave packet in this case, one may need several more eigenfunctions than for the δ case. Indeed, in the previous subsection we construct the initial wave packet with very good accuracy by using $N=102$. If we choose four δ' potentials all with $\gamma=120$, we will need $N=400$ to have Eq. (6) with an error of 5%. On the other hand, if we replace one of the δ''s by the usual δ potential, then we can built a Gaussian wave packet with a much smaller number of eigenfunctions, namely, $N=107$, with a precision of 10^{-12}.

Because of the large N necessary for four δ' potentials, we have investigated for this setup the rebuilding of the wave packet only for short times. By using the parameter values of Fig. 1, we observed basically the same type of revival. Indeed, at $t=0.955$, the wave packet rebuilds itself in the starting region II, as well as for $t=2\times 0.955$. Also, at $t=0.477$ it splits into two parts as in Fig. 1(c). For large times, the wave packet displays similar behavior to that seen in Fig. 2, bouncing between regions II and IV.

The case of three δ' and one δ reveals interesting features. For the case of $\delta'-\delta'-\delta-\delta'$, so that the initial wave packet (6) is between two δ' potentials, we find a very strong trapping effect. For instance, in Fig. 5 we show typical results for all the contact interactions γ equal to 10, $l_1=1$, $l_2=2.4$, $l_3=3.5$, $l_4=4.9$, $L=5$, and $k_0=21$. The particle stays confined in region II for all times. Here we should observe that the region lengths are no longer incommensurable and k_0 is relatively high.

If now we consider the configuration $\delta'-\delta-\delta'-\delta'$, then the initial wave packet is between a δ' and a δ potential. By using in this case the same parameters as in Fig. 5, the wave packet no longer remains confined in region II. It spreads out over regions II and III. The δ function at $x=l_3$ cannot retail the wave packet. On the other hand, by keeping all the parameters but setting the δ function $\gamma=120$ and $k_0=0$, then we have the evolution shown in Fig. 6. The wave packet spends most of its time within region II. There is some leakage, however, where the particle can be found in region III with a maximum probability of 11.2% [see Fig. 6(b)].

C. Asymmetric potentials

Next we consider the case where our four contact interaction potentials (all equal) are asymmetric. By asymmetric we mean that if one of the potentials is placed on the full line, the corresponding transmission and reflection amplitudes from the left are different from those from the right. This is achieved, for instance, by choosing $a=c=1/\gamma$, $b=0$, $d=\gamma$, $\theta=-\pi/2$, resulting from Eq. (7) in $R^{(\pm)}=[1\pm ik(\gamma^2-1)]/[-1+ik(\gamma^2+1)]$ and $T^{(\pm)}=\pm[2k\gamma]/[-1+ik(\gamma^2+1)]$.

Similarly to the δ' potentials, this case also shows a stronger trapping effect than that observed for the δ's. In fact, taking the same l_j's as the ones in Fig. 3 and setting $\gamma=10$ and the momentum $k_0=9$, in contrast to $k_0=0$ for the δ's, we see from Fig. 7 that the particle does not leave the initial region II (here, $N=110$ gives a precision better than 10^{-10} for the initial Gaussian wave packet). We have also tested the incommensurability condition. Again, we have verified that

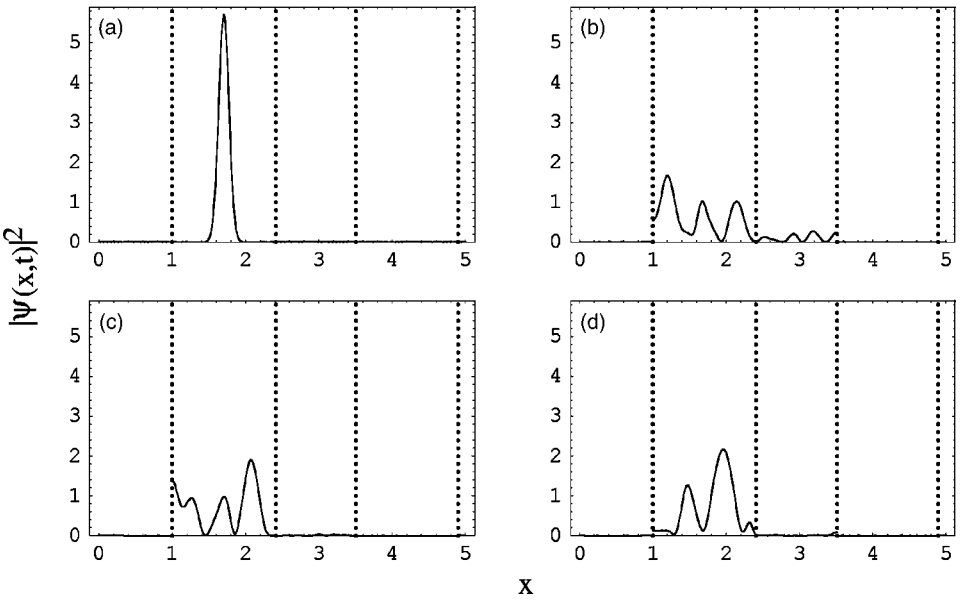

FIG. 6. The same as in Fig. 5, except for the different configuration $\delta' - \delta - \delta' - \delta'$, the δ function strength set to 120, and $k_0 = 0$. The times are (a) $t = 0$; (b) $t = 72$; (c) $t = 573$; (d) $t = 1705$. The confinement is not as strong as in Fig. 5. For instance, in (b) the probability for the particle to be found in region III is about 11%.

by taking irrational lengths to three decades the localization still holds. Leakage starts to appear for a two-decade approximation for the square roots.

D. Robin boundary condition–like potentials

As a final example, we turn to the case with all four contact interactions having the parameter values $a = 1$, $b = 1/\gamma$, $c = \gamma$, $d = 2$, and $\theta = 0$. Such values result in the following quantum coefficients for a single contact interaction on the line: $R^{(\pm)} = [(k^2 + \gamma^2) \pm ik\gamma]/[(k^2 - \gamma^2) + 3ik\gamma]$ and $T^{(\pm)} = T = 2ik\gamma/[(k^2 - \gamma^2) + 3ik\gamma]$. These R and T have a k^2 dependence, not present in the reflection and transmission amplitudes for the δ and δ' (see previous sections), nor for more usual potentials like step, rectangular, Rosen-Morse, and Woods-Saxon barriers [2,28].

The reason we pick this set of boundary conditions is twofold. First, we shall analyze the wave-packet time evolution for potentials that impose the so called Robin boundary conditions [29] on the wave function, i.e., ψ and ψ' just after the contact interaction depend on both ψ and ψ' just before the contact interaction [which is readily seen by putting the above parameters into Eq. (2)]. Second, these potentials are interesting on their own because they generate different phenomena in the context of quantum graphs (see, e.g., [14] and references therein).

We consider the same parameters as those in Fig. 1. Again, by using $N = 110$ we get a precision better than 10^{-10} for the initial state. The time evolution is shown in Fig. 8, where we see that the wave packet bounces between regions II and IV. Despite the fact that in this case the wave function and its first derivative are discontinuous at all $x = l_j$'s, we still have partial and (approximate) full revival in regions II and IV. We have also investigated the dynamics for increasing values of k_0. Up to $k_0 = 12$ the joint probability of being in the regions II and IV remains practically the unity. The patterns

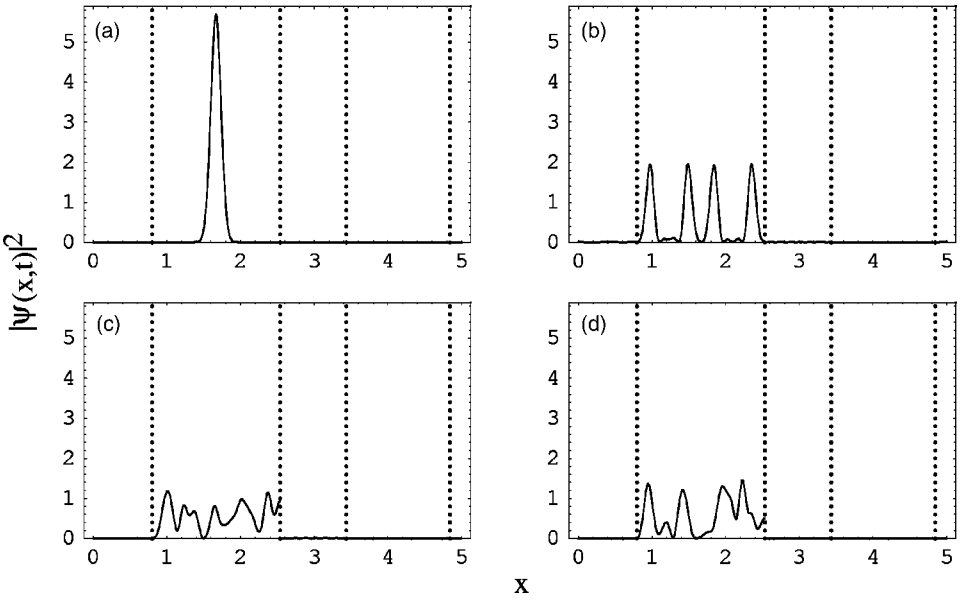

FIG. 7. The wave-packet time evolution for the asymmetric case. The times are (a) $t = 0$; (b) $t = 1.433$; (c) $t = 42.2$; and (d) $t = 5000$. The initial Gaussian has momentum $k_0 = 9$ and does not leave region II for any time.

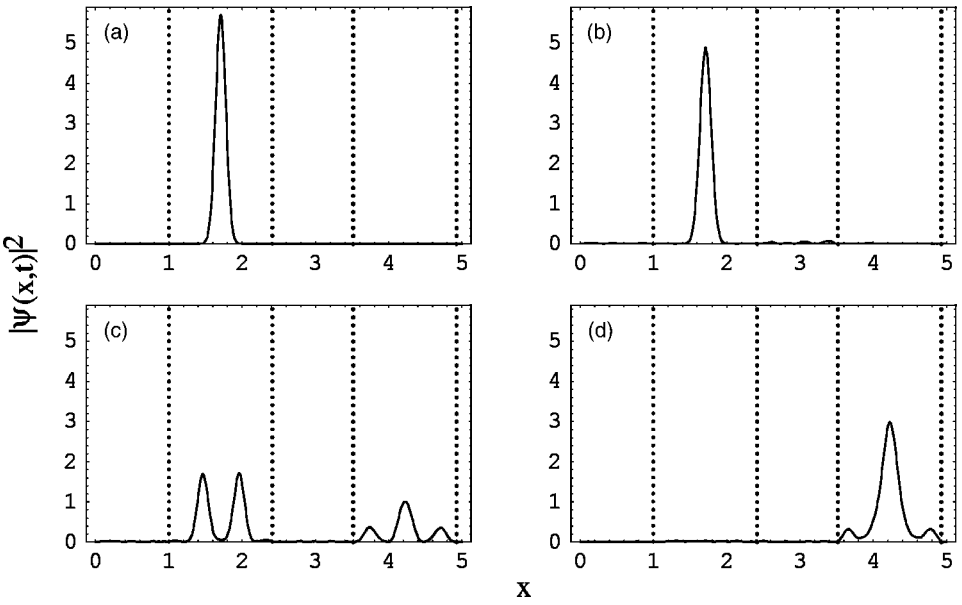

FIG. 8. $|\psi(x,t)|^2$ as a function of x for the Robin boundary condition–like potentials. Here, the times are (a) $t=0$; (b) $t=0.329$; (c) $t=75$; and (d) $t=563.924$. We observe approximately full revival in (b), partial revivals in regions II and IV in (c), and somewhat of a reconstruction at region IV in (d).

of partial and almost full revivals in regions II and IV are also not destroyed, but of course the revival times change according to k_0.

IV. REMARKS AND CONCLUSION

Here we discussed a simple but nevertheless instructive problem. We considered a finite 1D lattice, of length L, composed of four general contact interactions and under periodic boundary conditions. By setting different values for the parameters that characterize the contact potentials, we studied the time evolution of wave packets. They exhibited different behaviors, such as revivals, bouncing, and trapping. It is worth mentioning that, as far as we know, this work is a first effort to compare, for different cases, the effects of scattering of wave packets by sets of contact potentials.

To study the time evolution of our problem we used the standard expansion technique. As seen in most of the examples, for Gaussian wave packets we can truncate our series at relatively small N's. So the calculations are performed in a quite reasonable computational time. For some situations, however, the Fourier expansion may be slowly convergent, as for a Gaussian in a more singular setup for the system (e.g., the four-δ' setup in Section III B), or when the initial wave function has a more complicated shape. In these cases a possible alternative is to solve the time-dependent Schrödinger equation directly from well known numerical procedures like the splitting operator method. Another possibility, if instead of obtaining $\psi(x,t)$ one has interest only in determining particular quantities, is to try to develop analytical approaches. For instance, in Ref. [13] the authors discuss the problem of a δ function within an infinite square well. They are able to derive the revival times for wave packets that have components with very high quantum numbers. They do so by making analytical approximations of the transcendental equation of the eigenstates (resulting in explicit formulas for the k_n's in terms of the n's) and by exploring symmetry properties. Because of some similarity of our system with that in [13], in principle one could follow the same idea here. The only problem is that in our case the calculations are far more complicated, as one can grasp from a direct inspection of Eqs. (3) and (5), which are the quantization conditions for the simpler cases of four equal δ and δ' potentials, respectively.

As pointed out in the Introduction, the possibility of reproducing similar systems in the laboratory, with microwaves [22] or even with ultracold atoms [30], would be very useful in order to test and develop quantum evolution control techniques as well as to study fundamental phenomena in quantum physics. Indeed, by using the usual δ functions, we have shown that one can split an initially localized state into two parts considerably away from each other (see Fig. 4). If implemented, such a system could be used as a prototype of a "macroscopic quantum cat" or as a simpler realization of the much more complicated experiment on quantum mirages. We have also shown that, by using more singular contact interactions, as in the example of δ' potentials, the trapping and bouncing can be enhanced due to the stronger effects of these potentials in scattering off the wave packets. This would be desirable in order to measure the so called atomic mirror forces [31].

Finally, we mention that the present is an exploratory work. So we have considered only some particular sets of parameter values for just four contact interaction potentials which, however, have already shown rich dynamics. Making other parameter combinations and increasing the number of contact interactions may lead to many other interesting features for wave-packet time evolution in finite periodic lattices.

ACKNOWLEDGMENT

The authors gratefully acknowledge CNPq for financial support.

[1] I. Walmsley and H. Rabitz, Phys. Today **56**(8), 43 (2003).
[2] M. G. E. da Luz, B. K. Cheng, and M. W. Beims, J. Phys. A **34**, 5041 (2001); F. M. Andrade, B. K. Cheng, M. W. Beims, and M. G. E. da Luz, *ibid.* **36**, 227 (2003).
[3] D. L. Aronstein and C. R. Stroud, Jr., Phys. Rev. A **55**, 4526 (1997).
[4] D. L. Aronstein and C. R. Stroud Jr., Phys. Rev. A **62**, 022102 (2000).
[5] A. Venugopalan and G. S. Agarwal, Phys. Rev. A **59**, 1413 (1999).
[6] W. G. Harter, Phys. Rev. A **64**, 012312 (2001).
[7] R. Bluhm and V. A. Kostelecký, Phys. Lett. A **200**, 308 (1995); Phys. Rev. A **51**, 4767 (1995); A. Peres, *ibid.* **47**, 5196 (1993); J. A. Yeazell, M. Mallalieu, and C. R. Stroud, Phys. Rev. Lett. **64**, 2007 (1990).
[8] S. I. Vetchinkin and V. V. Eryomin, Chem. Phys. Lett. **222**, 394 (1994).
[9] B. M. Garraway and K-A. Suominem, Rep. Prog. Phys. **58**, 365 (1995); D. J. Tannor and S. A. Rice, J. Chem. Phys. **83**, 5013 (1985).
[10] I. Sh. Averbukh and N. F. Perelman, Phys. Lett. A **139**, 449 (1989).
[11] J. Banerji and G. S. Agarwal, Phys. Rev. A **59**, 4777 (1999); R. Bluhm, V. A. Kostelecký and J. A. Porter, Am. J. Phys. **64**, 944 (1996); S. Seshadri, S. Lakshmibala, and V. Balakrishnan, J. Stat. Phys. **101**, 213 (2000); D. J. Fernández and C. B. Mielnik, J. Math. Phys. **35**, 2083 (1994).
[12] Y. Ashkenazy, L. P. Horwitz, J. Levitan, M. Lewkowicz, and Y. Rothschild, Phys. Rev. Lett. **75**, 1070 (1995); L. P. Horwitz, J. Levitan, and Y. Ashkenazy, Phys. Rev. E **55**, 3697 (1997).
[13] G. A. Vugalter, A. K. Das, and V. A. Sorokin, Phys. Rev. A **66**, 012104 (2002).
[14] A. G. M. Schmidt, B. K. Cheng, and M. G. E. da Luz, J. Phys. A **36**, L545 (2003).
[15] A. G. M. Schmidt, B. K. Cheng, and M. G. E. da Luz, Phys. Rev. A **66**, 062712 (2002).
[16] H. Danared, J. Phys. B **17**, 2619 (1984); W. Däppen, *ibid.* **10**, 2399 (1977); G. Scheitler and M. Kleber, Phys. Rev. A **42**, 55 (1990).
[17] S. Albeverio, S. M. Fei, and P. Kurasov, Rep. Math. Phys. **47**, 157 (2001).
[18] T. Cheon and T. Shigehara, Phys. Rev. Lett. **82**, 2536 (1999); T. Cheon, T. Fülöp, and I. Tsutsui, Ann. Phys. (N.Y.) **294**, 25 (2001).
[19] C. Grosche, J. Phys. A **28**, L99 (1995); D. K. Park, J. Math. Phys. **36**, 5453 (1995); M. Carreau, J. Phys. A **26**, 427 (1993); F. A. B. Coutinho, Y. Nogami, and J. F. Perez, *ibid.* **30**, 3937 (1997).
[20] T. Cheon and T. Shigehara, Phys. Lett. A **243**, 111 (1998); T. Cheon, T. Shigehara, and K. Takayanagi, J. Phys. Soc. Jpn. **69**, 345 (2000); T. Shigehara, H. Mizoguchi, T. Mishima, and T. Cheon, IEICE Trans. Fundamentals **E82-A**, 1708 (1999).
[21] T. Fülöp, T. Cheon, and I. Tsutsui, Phys. Rev. A **66**, 052102 (2002).
[22] U. Kuhl and H.-J. Stöckmann, Physica E (Amsterdam) **9**, 384 (2001); U. Kuhl, F. M. Izrailev, A. A. Krokhin, and H.-J. Stöckmann, Appl. Phys. Lett. **77**, 633 (2000); U. Kuhl and H.-J. Stöckmann, Phys. Rev. Lett. **80**, 3232 (1998).
[23] S. Albeverio, F. Gesztesy, R. Hoegh-Krohn, and H. Holden, *Solvable Models in Quantum Mechanics* (Springer-Verlag, Berlin, 1988).
[24] M. Murakami, G. W. Ford, and R. F. O'Connell, Laser Phys. **13**, 180 (2003); A. Montina and F. T. Avecchi, Phys. Rev. A **66**, 013605 (2002); E. Solano, G. S. Agarwal, and H. Walther, Opt. Spectrosc. **94**, 805 (2003); G. S. Agarwal, R. R. Puri, and R. P. Singh, Phys. Rev. A **56**, 2249 (1997); K. Wodkiewicz, Opt. Commun. **179**, 215 (2000).
[25] H. C. Manoharan, C. P. Lutz, and D. M. Eigler, Nature (London) **403**, 512 (2000).
[26] A. Lobos and A. A. Ligia, Phys. Rev. B **68**, 035411 (2003).
[27] D. K. Park, J. Phys. A **29**, 6407 (1996); P. Exner and P. Šeba, Rep. Math. Phys. **28**, 7 (1989); P. Exner, M. Tater, and D. Vaněk, J. Math. Phys. **42**, 4050 (2001).
[28] S. Flügge, *Practical Quantum Mechanics* (Springer-Verlag, Berlin, 1974).
[29] K. E. Gustafson, *Introduction to Partial Differential Equations and Hilbert Space Methods* (Dover, Mineola, NY, 1999).
[30] F. Shimizu, Phys. Rev. Lett. **86**, 987 (2001).
[31] V. V. Dodonov and M. A. Andreata, Phys. Lett. A **275**, 173 (2000); Laser Phys. **12**, 57 (2002).